2026 International Conference on Sustainable Engineering and Digital Innovation (ICSEDI) | 979-8-3315-7563-2/26/$31.00 ©2026 IEEE | DOI: 10.1109/ICSEDI66420.2026.11568325

Temperature Prediction of a Photovoltaic Panel Integrated with Phase Change Material Using Machine Learning

Wisam K. Hussam
Mechanical Engineering, College of Engineering, Australian University, West Mishref, Safat 13015, Kuwait
w.alsaadi@au.edu.kw

Ahmad Bani Mustafa
Mathematics and Physics, College of Engineering, Australian University, West Mishref, Safat 13015, Kuwait
a.mustafa@au.edu.kw

Omar Ali Yousef
Mechanical Engineering, College of Engineering, Australian University, West Mishref, Safat 13015, Kuwait
o.yousef@au.edu.kw

Shehab Hasan AlShammari
Mechanical Engineering, College of Engineering, Australian University, West Mishref, Safat 13015, Kuwait
232200152@au.edu.kw

Gregory J. Sheard
Department of Mechanical and Aerospace Engineering, Monash University, Melbourne 3500, Australia
greg.sheard@monash.edu

***Abstract*—This study investigates the performance of a photovoltaic (PV) module integrated with a phase change material (PCM) layer by combining TRNSYS thermal simulations with several machine-learning regression models. The TRNSYS framework produced temperature and meteorological datasets for different PCM thicknesses, which were then used to train and assess Gaussian Process Regression (GPR), Support Vector Machine (SVM), and related models. The most accurate model was subsequently applied to examine the cooling effect introduced by the PCM layer and its influence on electrical output. Of the configurations evaluated, the 2 cm PCM layer delivered the most notable improvement, lowering the average module temperature by approximately 9.6 °C (17.2%) and increasing power generation by 22.1% relative to the reference module. For a representative 28 m^2 residential array of about 17 modules, the expected annual financial benefit ranges from roughly 70 USD under Kuwait's tariff to nearly 300 USD in higher-priced electricity markets. Overall, the results indicate that a 2 cm PCM layer offers a practical compromise between thermal management and economic value.**

***Index Terms*—Photovoltaic, PCM, Machine learning, TRNSYS**

I. Introduction

The electrical behaviour of a photovoltaic (PV) module is closely linked to the temperature at which it operates. An increase in cell temperature typically reduces the open-circuit voltage and strengthens resistive losses, which together diminish conversion efficiency. These temperature-induced effects become particularly significant in hot climatic regions, where PV modules often function well above standard test conditions (STC) for extended periods. As a result, maintaining acceptable operating temperatures is essential for sustaining output and limiting long-term thermal degradation.

A range of passive temperature-control strategies has been explored, among which phase change materials (PCMs) have shown consistent promise. During the melting process, PCMs absorb thermal energy through latent heat storage and thereby slow the temperature rise of the module during peak irradiance hours. Experimental investigations have reported measurable improvements in PV performance when PCM layers are installed at the rear of the module [1], [2]. Additional studies show that PCM behaviour is highly dependent on melting temperature, thermal conductivity, and its placement relative to the panel surface [3]. The amount of PCM is another important consideration: when the PCM layer is excessively thick, the remaining heat may not be fully released overnight, which limits solidification and reduces the cooling capacity available the following day [4].

Several researchers have also employed TRNSYS to evaluate PCM-integrated PV systems under realistic outdoor conditions. Comparisons between simulated and measured temperatures demonstrate that TRNSYS can reproduce the primary thermal trends of these systems with good accuracy [5], [6]. These studies also emphasise how PCM thickness and melting temperature affect daytime cooling and night-time thermal recovery.

In parallel with advances in PCM-based cooling, machine learning (ML) regression techniques have become increasingly useful for predicting PV module temperature. Such models can account for nonlinear interactions between solar irradiance, ambient temperature, wind conditions, and module properties, often achieving higher accuracy than empirical thermal models. Previous investigations show that algorithms such as Gaussian Process Regression and Support Vector Regression perform well under fluctuating weather conditions [7]. Other thermal analyses highlight the major role of convective heat transfer, especially wind-driven cooling, in determining PV module temperature [8], [9]. Studies conducted in semi-arid climates similarly emphasise the importance of models that reflect local environmental characteristics [10], [11].

Despite progress in both areas, PCM-enhanced PV systems and ML-based prediction methods have typically developed along separate lines. Most PCM research relies on experimental setups or stand-alone simulations, whereas many ML-based temperature studies examine conventional PV modules that do not include PCM layers. This limits opportunities to evaluate PCM behaviour under variable conditions or to apply ML-driven optimisation in PCM-integrated systems.

The present work addresses this gap by developing supervised ML regression models capable of forecasting the operating temperature of a PV module with PCM integration, using environmental and module-temperature data generated by TRNSYS. The main contributions of this study are summarised below:

- Construction of a TRNSYS model that represents the coupled thermal response of a PV–PCM module under varying environmental inputs.
- Training and evaluation of several ML regression models to identify an accurate temperature-prediction approach.
- Assessment of the thermal influence of PCM thickness using the trained model.
- Practical guidance for selecting PCM thickness for PV installations exposed to hot climates.

II. Material and Methodology

A. TRNSYS Simulation Model

A TRNSYS model was constructed to evaluate both the thermal behaviour and electrical output of the PV module when integrated with a phase change material (PCM) layer. The model configuration, illustrated in Fig. 1, employs Type 590, which represents an unglazed PV panel combined with a PCM layer. Within this component, the electrical output is determined from the overall module efficiency, and TRNSYS allows this efficiency to be provided in several forms. Depending on the available data, the user may specify a constant efficiency, a variable input, a data file that relates efficiency to cell temperature and solar irradiance, or a set of reference values with correction coefficients describing the influence of irradiance and temperature.

Type 590 provides four computational modes, each tailored to different levels of input detail. For the present work, the second approach was selected. In this mode, efficiency under reference test conditions is supplied together with its dependence on irradiance and temperature. This facilitates a direct coupling between environmental conditions, cell temperature, and the resulting electrical output. Hourly meteorological data for Kuwait City were obtained from Meteonorm and imported into TRNSYS to establish realistic boundary conditions for the simulations.

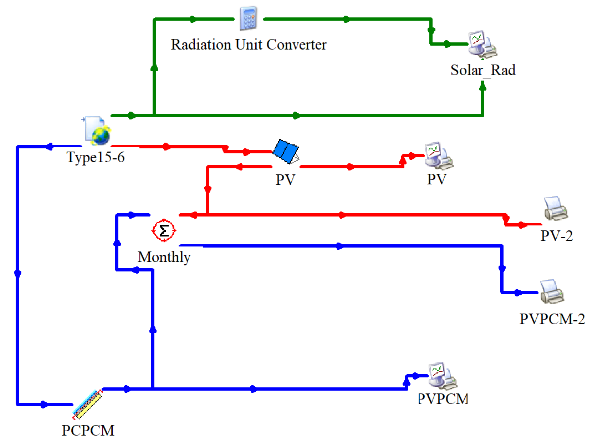

Fig. 1. TRNSYS Module configuration for computational modeling of integrated PV–PCM systems.

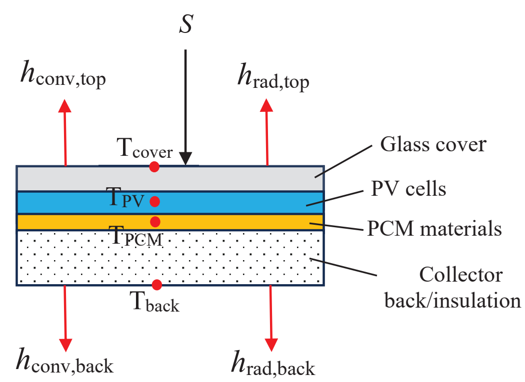

Fig. 2. Configuration of PV–PCM modules for TRNSYS-based modeling. solar irradiance S incident on the glass cover, with convective and radiative heat transfer at the top and back surfaces ($h_{\text{conv,top}}$, $h_{\text{rad,top}}$, $h_{\text{conv,back}}$, $h_{\text{rad,back}}$). The temperature nodes T_{cover}, T_{PV}, T_{PCM}, and T_{back} correspond to the cover, PV cells, PCM layer, and back insulation, respectively.

Fig. 2 shows the TRNSYS modeled PV–PCM configuration. Unlike glazed photovoltaic modules, which include a transparent front cover, the system used in this study is unglazed and therefore does not contain any glazing layer on the module surface.

The overall efficiency of the PV and the energy flux density produced by the PV-PCM module are calculated, respectively, as [5], [21]

$$\eta = [1 + \eta_{T,\text{coef}}(T_{\text{PV}} - T_{\text{ref}})] \times [1 + \eta_{I,\text{coef}}(I_T - I_{T,\text{ref}})]\,\eta_{\text{ref}}. \quad (1)$$

$$P_{\text{PV}} = (\tau\alpha)_n (IAM) I_T \eta A, \quad (2)$$

where η is the overall efficiency of the PV panel, η_{ref} is the efficiency under reference conditions, and $\eta_{T,\text{coef}}$ is the temperature coefficient of efficiency. T_{PV} denotes the PV cell temperature, while T_{ref} is the reference temperature. $\eta_{I,\text{coef}}$ represents the irradiance coefficient of efficiency, I_T is the total incident solar radiation, and $I_{T,\text{ref}}$ is the reference solar radiation. Additionally, P_{PV} is the energy flux density (power) produced by the PV panel, $(\tau\alpha)_n$ is the transmittance-absorptance product of the PV cover, IAM is the incidence angle modifier, and A is the surface area of the PV panel. Using equations (1) and (2), one can determine the overall efficiency and electrical power output of the PV-PCM system.

The temperature of the PV cell is governed by the energy balance among the various layers of the PV-PCM panel, which depends on the incident solar radiation and the heat transfer mechanisms occurring within the panel. Energy balance equations [5], [6] are critical in systems where heat transfer and temperature fluctuations are dominant factors. Accordingly, the thermal equilibrium at each layer including the PV panel's top surface, the photovoltaic cells, the phase-change material (PCM) section, and the rear surface is quantified by equations (3)-(6).

$$\frac{T_{\text{PV}} - T_C}{R_1} = h_{\text{conv,top}}(T_C - T_{\text{amb,top}}) + h_{\text{rad,top}}(T_C - T_{\text{rad,top}}), \tag{3}$$

$$S = \frac{T_{\text{PV}} - T_C}{R_1} + \frac{T_{\text{PV}} - T_{\text{PCM}}}{R_2}, \tag{4}$$

$$mc_p \frac{dT_{\text{PCM}}}{dt} = \frac{T_{\text{PV}} - T_{\text{PCM}}}{R_2} - \frac{T_{\text{PCM}} - T_B}{R_3}, \tag{5}$$

$$\frac{T_{\text{PCM}} - T_B}{R_3} = h_{\text{conv,back}}(T_B - T_{\text{amb,back}}) + h_{\text{rad,back}}(T_B - T_{\text{rad,back}}), \tag{6}$$

where R_1 is the thermal resistance of the transparent sheet, $h_{\text{conv,top}}$ is the top surface convection heat transfer coefficient, $h_{\text{rad,top}}$ is the radiation heat transfer coefficient of the top surface, T_C is the cover temperature, R_2 is the thermal resistance of the PV cells, m is the PCM mass, C_p is the specific heat capacity, R_3 is the thermal resistance of the back sheet, T_B is the back sheet temperature, $h_{\text{conv,back}}$ is the back surface convection heat transfer coefficient, $h_{\text{rad,back}}$ is the radiation coefficient of the back surface, $T_{\text{amb,back}}$ is the ambient temperature for convective losses, and $T_{\text{rad,back}}$ is the radiative sink temperature.

The total energy required to fully melt of fully solidify the PCM material is given as

$$Q_{\text{sol}} = Q_{\text{liq}} = mh_{\text{fg}}, \tag{7}$$

where h_{fg} denotes the PCM's latent heat of fusion, with $Q_{\text{sol}} = Q_{\text{liq}}$ indicating the equal magnitude of specific energy required for complete phase transformation between 100% solid and 100% liquid states.

The technical specifications of the PV module and thermophysical properties of the PCM used in this study are provided in Tables (I) and (II), respectively.

TABLE I
SPECIFICATIONS OF THE CS6P-250M PV MODULE

Parameter	Value
Module type	CS6P-250M
Maximum power, P_{mp}	$250\,\text{W}$
Maximum power voltage, V_{mp}	$30.4\,\text{V}$
Maximum power current, I_{mp}	$8.22\,\text{A}$
Open circuit voltage, V_{oc}	$37.5\,\text{V}$
Short circuit current, I_{sc}	$8.74\,\text{A}$
Module efficiency	15.54%
Temperature coefficient of P_{mp}	$-0.45\%/^\circ\text{C}$
Temperature coefficient of V_{oc}	$-0.35\%/^\circ\text{C}$
Temperature coefficient of I_{sc}	$+0.06\%/^\circ\text{C}$
Cell technology	Monocrystalline silicon
Number of cells	60 (6×10)
Module dimensions	$1639 \times 982 \times 40\,\text{mm}$

TABLE II
THERMAL PROPERTIES OF THE PCM [12].

Thermal Property	Value
Melting peak (°C)	30.5
Latent heat of fusion (kJ/kg)	245
Thermal conductivity (W/m·K)	0.2
Density (kg/m^3)	920
Specific heat capacity (kJ/kg·K)	2

B. Machine Learning Model

Before model training, the TRNSYS outputs were prepared to match the machine-learning data structure. The simulations used a 0.25 h time step, and the results were aggregated to hourly resolution for consistency with the predictor variables. The MATLAB Regression Learner App was used with its default preprocessing, which automatically normalises the input variables. Because the dataset was generated numerically, no additional outlier filtering was required. Model evaluation employed five-fold cross-validation to ensure balanced representation of all PCM thickness configurations.

Machine learning (ML) techniques were employed to support temperature prediction by learning the relationship between environmental variables and PV response. In general terms, ML models aim to construct data representations that allow accurate prediction of unknown outputs from known inputs [13]. Developing these representations is central to the learning process, and the suitability of a particular model depends on its ability to capture patterns that generalise well beyond the training dataset [14].

ML algorithms are typically categorised into supervised, unsupervised, and semi-supervised learning [15]–[17]. For PV applications, supervised learning is commonly selected because temperature and power output are continuous, measurable quantities. Among the available models, Support Vector Machines (SVMs) have shown strong performance, particularly in settings where nonlinear and high-dimensional relationships between climate variables and PV performance must be modelled [18].

In this study, supervised regression methods were used to describe the mapping between the predictor variables—such as global horizontal irradiance (GHI), ambient temperature (T_a), and PCM configuration—and the response variables: PV cell temperature and electrical power. These models learn functional relationships directly from the TRNSYS-generated dataset, enabling them to provide temperature and power predictions across a range of PCM thicknesses and climatic conditions [12].

III. Results and Discussion

In this work, meteorological input data and PV module temperatures generated in TRNSYS for different PCM thicknesses were used to train machine learning regression models. The trained models were then used to predict the module temperature for each PCM configuration and determine the optimal PCM thicknes that minimizes the PV operating temperature.

A. Climatic conditions of the study region

Kuwait is located in the northwestern part of the Gulf Cooperation Council (GCC) region and is characterized by an arid desert climate with high solar irradiance throughout the year. Clear-sky conditions dominate, with only limited rainfall or cloud-cover periods. Ambient temperatures usually exceed 50 °C during the summer months (May–September), resulting in substantial thermal loading on PV modules. These conditions highlight the need for effective thermal management system to mitigate temperature rise and maintain PV performance [19], [20].

B. Simulation results

The effect of PCM thickness on PV temperature and electrical power is presented in Figs. (3) and (4). Seasonal variability is evident: both temperature and power follow trends dictated by ambient temperature (T_a) and solar irradiance (GHI). In months with intense irradiance, PCM integration reduces the peak operating temperature of the module. The 2 cm PCM layer provides the most consistent cooling across summer months, followed by the 1 cm layer. The 3 cm configuration exhibits diminished effectiveness due to incomplete resolidification during night-time periods. Compared with the baseline (0 cm), the 1 cm PCM layer yields a 4.95 °C reduction and an 18.8% power increase, while the 2 cm layer achieves a 9.55 °C reduction and a 22.1% power gain. The 3 cm layer exhibits only slight additional cooling (10.5 °C) and a marginal rise in power output (22.8%), confirming that excessive PCM thickness can limit daily thermal recovery.

Figs. (3) and (4) present the influence of PCM layer thickness on the monthly average PV module temperature and power output obtained from the TRNSYS simulations. Both quantities follow the expected seasonal trends imposed by ambient temperature (T_a) and global horizontal irradiance (GHI). During the high-irradiance summer months, the inclusion of PCM lowers the module temperature noticeably, with the 2 cm layer showing the strongest reduction. The 1 cm layer also improves performance, whereas the 3 cm layer becomes less effective due to its tendency to retain heat and its limited ability to fully resolidify overnight.

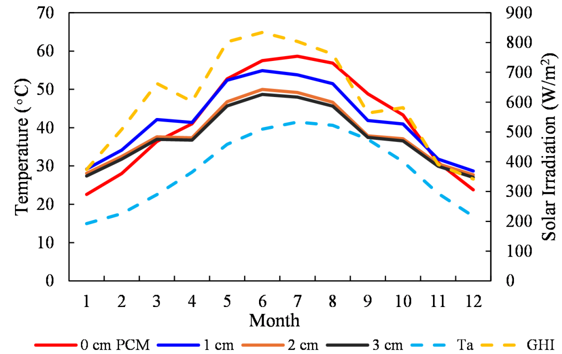

Fig. 3. Monthly average PV temperature for different PCM thickness, including reference curves for ambient temperature $\mathrm{T_a}$ and global horizontal radiation GHI. Month numbers represent January through to December.

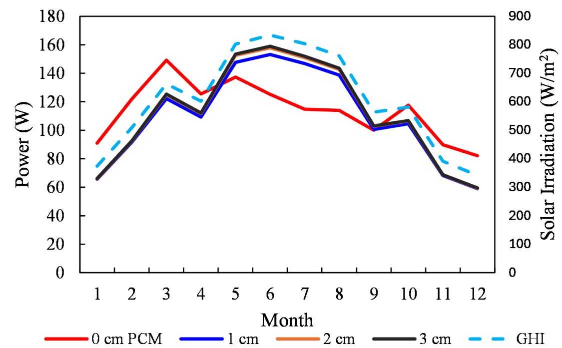

Fig. 4. Monthly average power for different PCM thickness, including reference curves for ambient temperature $\mathrm{T_a}$ and global horizontal radiation GHI. Month numbers represent January through to December.

Relative to the 0 cm reference case, the 1 cm PCM layer reduces the average module temperature by $4.95°\mathrm{C}$ (8.9%) and increases power output by 18.8%. The 2 cm configuration provides the most substantial effect, reducing temperature by $9.55°\mathrm{C}$ (17.2%) and enhancing power by 22.1%. The 3 cm layer yields only a slightly greater temperature decrease ($10.5°\mathrm{C}$, 18.9%) and a small additional rise in power (22.8%), indicating diminishing returns linked to incomplete night-time solidification. Overall, the simulations show that a 2 cm PCM layer offers the most favourable balance between cooling capability and electrical improvement under summer conditions.

C. Machine learning model performance

A range of machine learning algorithms were developed and assessed to determine their suitability for predicting PV module temperature. These included linear regression, SVM with a Gaussian kernel, SVM with a least-squares kernel, GPR with a squared exponential kernel, and GPR with a Matern $5/2$ kernel. Their comparative performance is summarised in Table I. As shown, the two GPR models provide the highest level of accuracy, with the GPR (Matern $5/2$) configuration

TABLE III
HOT-SEASON (JUN–SEP) IMPROVEMENT IN PV MODULE TEMPERATURE AND POWER RELATIVE TO THE 0 CM BASELINE.

PCM thk.	ΔT (°C)	Temp. drop (%)	ΔP (W)	Power gain (%)
1 cm	4.95	8.9	76.7	18.8
2 cm	9.55	17.2	90.4	22.1
3 cm	10.50	18.9	93.1	22.8

TABLE IV
COMPARISON OF MACHINE LEARNING MODELS FOR THE TEMPERATURE PREDICTION

Model	RMSE	MAE	R^2	MSE
Linear Regression	3.6783	3.0355	0.9138	13.5300
SVM (Gaussian Kernel)	2.0247	1.4617	0.9743	4.0996
SVM (Least-Squares Kernel)	1.8975	1.4168	0.9774	3.6004
GPR (Squared Exponential)	1.0973	0.6423	0.9924	1.2041
GPR (Matern 5/2)	0.9396	0.4970	0.9945	0.8829

achieving the lowest error metrics—an RMSE of 0.9396 and an MAE of 0.4970—together with the strongest coefficient of determination ($R^2 = 0.9945$). The linear regression model, by contrast, performs considerably worse because its structure cannot represent the nonlinear thermal interactions that govern PV module temperature.

The scatter plot in Fig. 5 provides additional evidence of the strength of the GPR (Matern $5/2$) model. The predicted temperatures cluster tightly around the 1:1 reference line, demonstrating close agreement with the TRNSYS outputs and indicating that the residual error is small across the full range of operating conditions. Owing to this level of predictive reliability, the GPR (Matern $5/2$) model was subsequently applied to estimate the thermal behaviour of the PV module for various PCM layer thicknesses and to identify the configuration that most effectively reduces the module operating temperature.

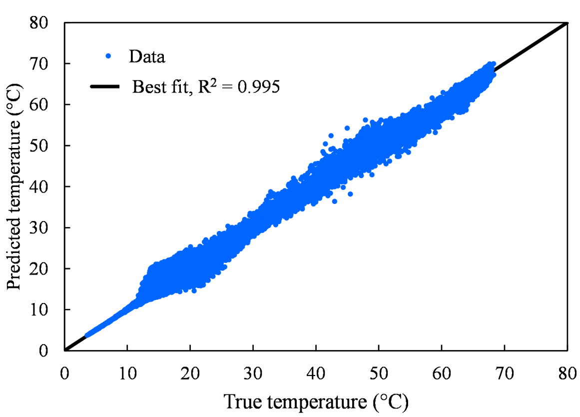

Fig. 5. Scatter plot for the Matern $5/2$ GRR ML model's predicted temperature versus TRNSYS data.

TABLE V
SEASONAL RECOMMENDATION FOR PCM THICKNESS BASED ON PREDICTED T_{pv}

Season	**Thickness**	**Rationale**
Hot (Jun–Sep)	2 cm	Provides strong cooling while allowing full melt/solidification cycles overnight.
Cold/Mild (Oct–May)	0 cm	Thermal load is low; PCM rarely melts, so added material provides no benefit.

D. PCM thickness optimization

Using the selected GPR (Matern $5/2$) model, T_{pv} was estimated for each PCM configuration (0–3 cm) throughout the year and examined on a seasonal basis. The predicted temperatures were compared across all months, and the PCM thickness that consistently produced the lowest operating temperature was identified as the optimal choice.

The results display a pronounced seasonal pattern, as summarized in Table V. During the hot season (June–September), when both T_a and GHI reach their maximum values, the 2 cm PCM layer provides the largest temperature reduction. This thickness offers adequate latent heat storage to absorb daytime thermal loads while still allowing full re-solidification during night-time hours, which is necessary to maintain cooling effectiveness on successive days. The 1 cm layer offers some thermal moderation but lacks sufficient storage capacity to match the performance of the 2 cm configuration.

By contrast, the 3 cm PCM layer performs less effectively despite its larger theoretical heat capacity. The increased thermal mass slows the release of stored heat, and the PCM does not consistently re-solidify overnight. As a result, a portion of the PCM begins the following day in a partially melted state, reducing the available cooling capacity and leading to higher operating temperatures compared with the 2 cm layer during extended hot periods.

In the cold and mild season (October–May), the thermal demand on the PV module is much lower, and PCM melting occurs infrequently. Under these conditions, the presence of PCM offers little benefit, and the 0 cm configuration performs comparably to the PCM-based cases. Consequently, PCM cooling is primarily effective under high thermal loading, when the phase-change cycle is active and able to reset between days.

E. Economic Evaluation

A cost–benefit assessment was carried out to estimate the economic implications of integrating PCM based on the additional energy produced during the hot season (June–September). For the recommended 2 cm PCM configuration, the TRNSYS–ML analysis predicts an average power enhancement of 90.4 W per module. Over the four-month period, and assuming an average of 8 h of daily operation, this improvement corresponds to an annual energy gain of approximately $88.15\ \mathrm{kWh/yr}$. When normalised by the module area of $1.6095\ \mathrm{m}^2$, the result is equivalent to $54.78\ \mathrm{kWh/m^2/yr}$.

To quantify the economic value of this additional energy, annual savings were estimated for a range of electricity tariff scenarios. Under Kuwait's current residential rate of \$0.046/kWh, the added energy yields a saving of roughly \$4.06 per module, or \$2.52 per m^2·yr. In regions with higher electricity prices, the benefit becomes more substantial; for example, tariffs of \$0.15/kWh (southern USA) and \$0.253/kWh (southern Australia) correspond to annual savings of approximately \$13.22 and \$22.32 per module, respectively.

For a typical residential installation covering 28 m^2 (approximately 17 modules), the results translate to total annual savings between \$69 in Kuwait and around \$380 in Australia. Although the financial return in Kuwait remains modest due to subsidised electricity pricing, the thermal mitigation afforded by the PCM layer provides clear technical advantages by lowering operating temperature and improving PV performance during extreme summer conditions. In higher-tariff markets, the same performance improvement leads to markedly larger economic gains, reinforcing the suitability of PCM integration for PV systems operating in hot and high-irradiance environments. Overall, the 2 cm PCM layer offers an effective balance between cooling capability, enhanced energy yield, and economic feasibility across the examined scenarios.

IV. Conclusion

This work examined the thermal and electrical behaviour of a photovoltaic module incorporating a phase change material layer under hot desert operating conditions. A TRNSYS model was used to simulate module temperature and power output for several PCM thicknesses, and the resulting dataset served as the basis for training a set of machine-learning regression models. The simulations showed that integrating PCM can reduce the operating temperature of the module, particularly during periods of intense solar irradiance. Among the tested configurations, the 2 cm PCM layer consistently provided the greatest benefit, lowering the temperature by up to 10.5 °C and increasing the power output by approximately 93 W at peak conditions.

The GPR model developed in this study demonstrated high predictive accuracy and was applied to assess the seasonal behaviour of each PCM thickness. The findings indicate that effective cooling requires the PCM to undergo a full melt–solidification cycle; this condition is reliably met by the 2 cm layer but not by thicker layers, which tend to retain heat and limit their ability to regenerate cooling capacity. For a typical 28 m^2 residential PV installation, the predicted improvement corresponds to an annual energy increase of around 1.5 MWh. While the financial benefit in Kuwait remains modest due to subsidised electricity prices, the technical gains are substantial, and the economic return becomes considerably more attractive in regions with higher tariffs.

Overall, the results show that a 2 cm PCM layer offers a practical and effective balance between temperature reduction, enhanced power output, and economic relevance for PV systems operating in hot, high-irradiance environments.

Future work may focus on validating these findings through experimental work to confirm the simulated temperature and power trends. Extending the analysis to different climatic regions would also help assess the variation in optimal PCM thickness under different weather conditions.

Acknowledgment

The authors gratefully acknowledge the support provided by the Mechanical Engineering Department at the Australian University of Kuwait.

References

[1] H. Shawish, M. Özdenefe, and S. Erdem, "Performance investigation and machine learning modeling of pv panels equipped with pcm based passive cooling systems," *Applied Thermal Engineering*, p. 126588, 2025.

[2] A. Shaito, M. Hammoud, F. Kawtharani, A. Kawtharani, and H. Reda, "Power enhancement of a pv module using different types of phase change materials," *Energies*, vol. 14, no. 16, p. 5195, 2021.

[3] M. A. Mohammed, B. M. Ali, K. F. Yassin, O. M. Ali, and O. R. Alomar, "Comparative study of different phase change materials on the thermal performance of photovoltaic cells in iraq's climate conditions," *Energy Reports*, vol. 11, pp. 18–27, 2024.

[4] D. Mazzeo *et al.*, "Integration of photovoltaic modules with phase change materials: Experimental testing, model validation and optimization," *Energy*, vol. 319, p. 134959, 2025.

[5] R. Stropnik and U. Stritih, "Increasing the efficiency of pv panel with the use of pcm," *Renewable Energy*, vol. 97, pp. 671–679, 2016.

[6] M. Rezvanpour, D. Borooghani, F. Torabi, and M. Pazoki, "Using cacl2· 6h2o as a phase change material for thermo-regulation and enhancing photovoltaic panels' conversion efficiency: Experimental study and trnsys validation," *Renewable Energy*, vol. 146, pp. 1907–1921, 2020.

[7] F. Bayrak, "Prediction of photovoltaic panel cell temperatures: Application of empirical and machine learning models," *Energy*, vol. 323, p. 135764, 2025.

[8] C. Schwingshackl *et al.*, "Wind effect on pv module temperature: analysis of different techniques for an accurate estimation," *Energy Procedia*, vol. 40, pp. 77–86, 2013.

[9] K. Boudjelthia *et al.*, "Role of the wind speed in the evolution of the temperature of the pv module: comparison of prediction models," *Journal of Renewable Energies*, vol. 19, pp. 119–126, 2016.

[10] I. Lamaamar *et al.*, "Evaluation of different models for validating photovoltaic cell temperature under semi-arid conditions," *Heliyon*, vol. 7, p. e08534, 2021.

[11] P. Trinuruk, C. Sorapipatana, and D. Chenvidhya, "Estimating operating cell temperature of bipv modules in thailand," *Renewable Energy*, vol. 34, pp. 2515–2523, 2009.

[12] A. Sedaghat, R. Kalbasi, A. Mostafaeipour, and M. Nazififard, "Practical application of machine learning in energy and thermal management: Long-term data analysis of solar-assisted ac systems in portable cabins in kuwait and australia," *Renewable Energy*, vol. 237, p. 121539, 2024.

[13] A. Mellit and S. Kalogirou, "Assessment of machine learning and ensemble methods for fault diagnosis of photovoltaic systems," *Renewable Energy*, vol. 184, pp. 1074–1090, 2022.

[14] F. Bayrak, "Prediction of photovoltaic panel cell temperatures: Application of empirical and machine learning models," *Energy*, vol. 323, p. 135764, 2025.

[15] Z. Razaghi-Moghadam and Z. Nikoloski, "Supervised learning of gene-regulatory networks based on graph distance profiles of transcriptomics data," *NPJ systems biology and applications*, vol. 6, no. 1, p. 21, 2020.

[16] D. C. Pagan, T. Q. Phan, J. S. Weaver, A. R. Benson, and A. J. Beaudoin, "Unsupervised learning of dislocation motion," *Acta Materialia*, vol. 181, pp. 510–518, 2019.

[17] J. E. Van Engelen and H. H. Hoos, "A survey on semi-supervised learning," *Machine learning*, vol. 109, no. 2, pp. 373–440, 2020.

[18] C. Idogho, E. O. Abah, J. O. Onuhc, C. Harsito, K. Omenkaf, A. Samuel, A. Ejila, I. P. Idoko, and U. E. Ali, "Machine learning-based solar photovoltaic power forecasting for nigerian regions," *Energy Science & Engineering*, vol. 13, no. 4, pp. 1922–1934, 2025.

[19] W. K. Hussam, H. J. Salem, A. M. Redha, A. M. Khlefat, and F. Al Khatib, “Experimental and numerical investigation on a hybrid solar chimney-photovoltaic system for power generation in kuwait,” *Energy Conversion and Management: X*, vol. 15, p. 100249, 2022.

[20] A. Sedaghat, K. Khanafer, R. Kalbasi, and A. Al-Masri, “A new approach for selecting and implementing phase change materials in kuwaiti buildings: Practical considerations,” *Journal of Energy Storage*, vol. 88, p. 111477, 2024.

[21] W. K. Hussam, A. M. Khlefat, and G. J. Sheard, “Energy saving and performance analysis of air-cooled photovoltaic panels,” *International Journal of Energy Research*, vol. 46, pp. 4825–4834, 2022.